1 The atmospheric boundary layer over glaciers

An atmospheric boundary layer is present everywhere. It is generally defined as the part of the atmosphere that is directly influenced by the surface. This influence derives from the exchange of momentum (friction), heat and moisture at the surface. In contrast to the free atmosphere, the structure of the boundary layer exhibits a marked daily cycle. At high latitudes, however, this is not necessarily the case because tha daily cycle in the surface fluxes can be quite small. For instance, katabatic flows over Antarctica in wintertime do not have a clear daily cycle. Yet these flows should be considered as boundary layer flows in which surface friction and the turbulent sensible heat flux are important components of the momentum and heat budget. In a way the same situation is found over melting glacier surfaces. During a large part of the summer temperature and vapour pressure at the surface have no daily cycle. Therefore the forcing of a glacier boundary layer from below is fairly constant and variations in its structure will be related to what happens higher up (Hoinkes, 1954).

In *figure 1* a typical summer time situation in a glacierised mountain region is sketched. Mountains appears as large roughness elements to the synoptic-scale atmospheric flow and a large-scale boundary layer will be present. In the valleys the diurnal rhythm of the valley/mountain wind system dominates the flow. It interacts with the large-scale boundary layer in a complex way. The glacier wind is a tiny element of this system but nevertheless regulates the turbulent fluxes to or from the glacier surface.

Balloon ascents have made it clear that the glacier wind is rather shallow, normally only some tens of metres. Measurements have also shown that it does not penetrate very far into the valley. At the point where the valley and glacier wind meet a weak front is present (indicated by F in *figure 1*). On really warm summer days the valley wind can become so strong that it erodes the glacier wind on the lower part of the glacier: the front moves upwards. This has been observed on several occasions on Austrian glaciers and on the Morteratschgletscher.

Figure 2 shows one year of-half hourly values of wind speed against wind direction and air temperature from the AWS on the Morteratschgletscher (Oerlemans and Grisogono, 2002). The fall line of the glacier is indicated by the arrow. Similar scatter plot for an AWS in the melting zone of the Greenland ice sheet (western Greenland near Kangerlussuaq) are shown in *figure 3*. A few things can be noted. First of all it appears that there is a strongly preferred wind direction. For the Morteratsch AWS this direction is along the fall line, making it very likely that the flow is of katabatic origin most of the time. In the melting zone of Greenland there appears to be a small shift of the preferred wind direction with respect to the fall line. This is a consequence of the Coriolis acceleration. In the case of Greenland the scale of the flow is sufficiently large to see

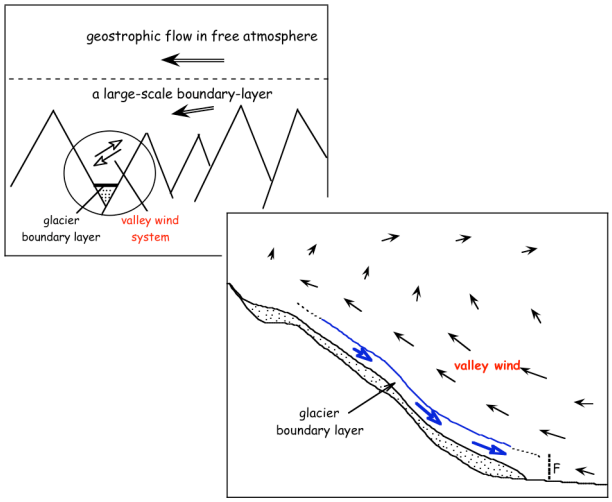

Figure 1. The basic structure of atmospheric circulation in a glacierised mountain region.

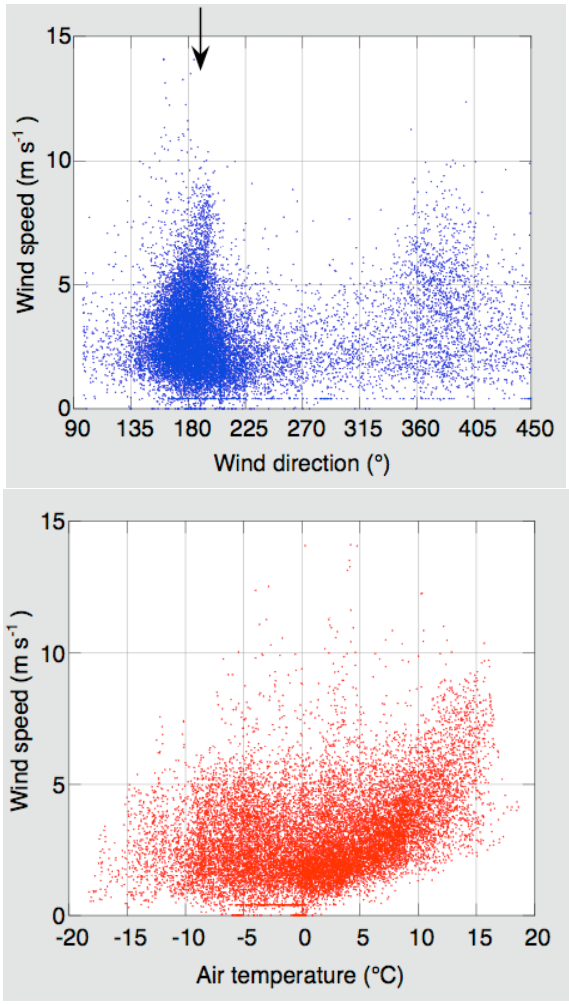

Figure 2. Plots of wind speed versus wind direction and air temperature from the AWS on the Morteratschgletscher. All half-hourly values for one year are shown.

the Coriolis effect.
As we will see later, the forcing of pure katabatic flow is proportional to the air temperature with respect to the ambient air temperature. During the ablation season the surface temperature is about 0°C, and the air temperature measured at some height therefore is a measure of the katabatic forcing. A relation between wind speed and temperature should therefore be expected when air temperature is above the melting point. In *figures 2-3* it can be seen that this is indeed the case.

2 Turbulent fluxes

Turbulent fluxes play an important role in shaping boundary layers. They also account for a significant part of the energy transfer between glacier surface and atmosphere. There are many textbooks about the atmospheric boundary layer and turbulence which give thorough treatments of the theory (e.g. Stull, 1988).
In a first approximtaion turbulent fluxes over glaciers (sensible heat: H_{se}, latent heat H_{la}, momentum: H_{mo}) can be described by the bulk equations:

$$H_{se} = \rho\, c_p C_{se}\, u\, (T - T_s) \qquad (2.1)$$

$$H_{la} = \rho\, L_v\, C_{la}\, u\, (q - q_s) \qquad (2.2)$$

$$H_{mo} = \rho\, C_d\, u^2 \qquad (2.3)$$

Here ρ is air density, c_p is the specific heat of air, L_v is the latent heat of vapourisation; u, T and q are the wind speed, temperature and specific humidity at the reference level; T_s and q_s are temperature and humidity at the surface. The turbulent exchange coefficients are denoted by C_{se}, C_{la} and C_d (the latter is also referred to as the drag coefficient). Note that the exchange coefficients are dimensionless.
It is important to remember that the constants C_{se}, C_{la} and C_d depend on the height at which the measurements are made. In fact, they should be considered as empirical constants that depend on the nature of the turbulence and, consequently, on the general atmospheric conditions and the roughness. Values found from field experiments are in the 10^{-2} to 10^{-4} range. In general values of C_{se} and C_{la} are rather similar, whereas the value for C_d tends to be larger. This is because part of the momentum transfer to the surface takes place through dynamic pressure differences across the obstacles (form drag), a process having no equivalent in the transfer of heat and water vapour.
The equations (2.1)-(2.3) are valid for neutral conditions. When the atmosphere is not neutrally stratified but is stably stratified (potential temperature increases with height) or unstably stratified (potential temperature decreases with

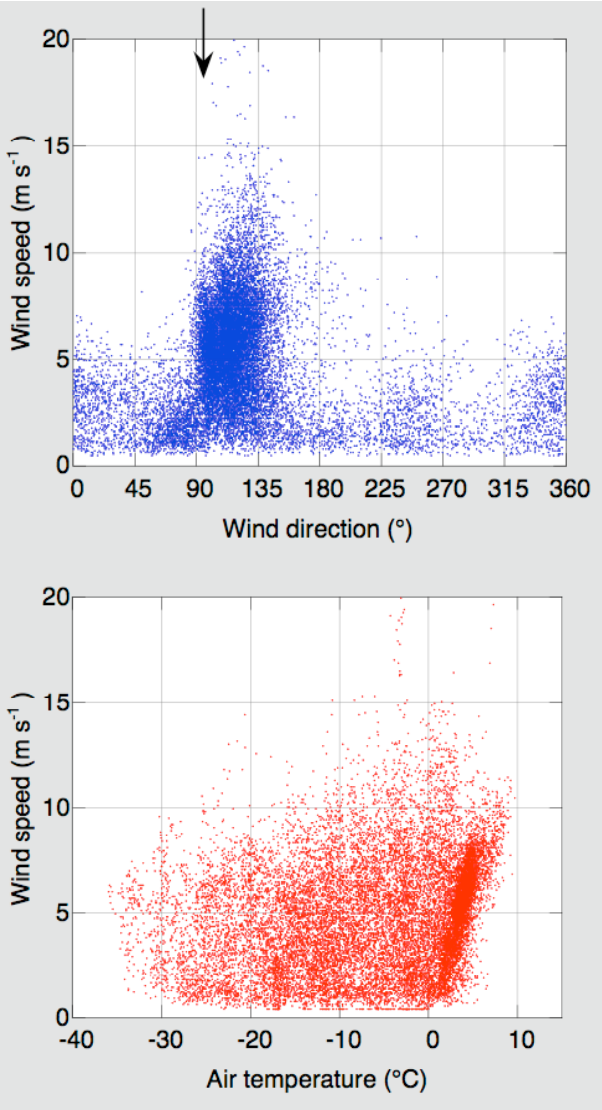

Figure 3. As in figure 2 but now for an AWS on the west Greenland ice sheet.

height), the scheme to calculate the fluxes is normally modified by applying Monin-Obukov similarity theory (Stull, 1988). With regard to the turbulent fluxes of heat and water vapour the major implication is that fluxes are suppressed in stable conditions and enlarged in unstable conditions. Since the temperature and wind profiles themselves depend on the fluxes, it is now more complicated to determine the fluxes from measurements (Munro and Davies, 1978). In the first place, measurements are needed from at least two levels. Secondly, some kind of iterative procedure has to be used.

Over melting glacier surfaces, the application of MO-theory turns out to be problematical. Because of the large stability (temperature gradients of the order of 1 K m-1) and the rough surface there is a zero-referencing problem: the fluxes and surface roughnesses determined by MO-theory become very dependent on how the height of the instruments is defined (Munro, 1989). This is an undesirable situation. It appears that the use of bulk equations in combination with a method for determining the surface roughness (*figure 4*) with a microtopographic method yield satisfactory results, and our discussion will be continued along these lines.

A possible relation between the drag coefficient and the root-mean-square surface topography σ_{surf} is

$$C_d = (1.10 + 0.72\sigma_{surf}) \times 10^{-3} \qquad (2.4)$$

Eq. (2.4) is one of the possible relations that have been suggested in the literature. It is based on a large number of measurements over various types of sea ice (Banke et al., 1980). Normally the drag coefficient is defined for $z_{ref} = 10$ m. If wind speed is measured at a different height z, the logarithmic wind profile can be used to convert the value for C_d to this height

$$C_d(z) = \frac{1}{C_d^{-1/2} - \kappa \ln(z_{ref}/z)} \qquad (2.5)$$

Among others, Andreas (1987) studied the relation between C_{se}, C_{la} and C_d. First of all he concluded that in most circumstances $C_{se} \approx C_{la}$. Then the relation he found between C_d and the heat exchange coefficients can be summarised as

$$C_{se} = C_d - \frac{C_d - 10^{-3}}{0.5\pi} \arctan(0.15u), \qquad (2.6)$$

where u is in m s^{-1}.

It is instructive now to compare how C_d and C_{se} vary with the topographic roughness σ_{surf} (*figure 5*). The variation is linear for given wind speed, as is obvious from eqs. (2.5) and (2.6). In fact, C_d is independent of the wind speed whereas C_{se} decreases with wind speed.

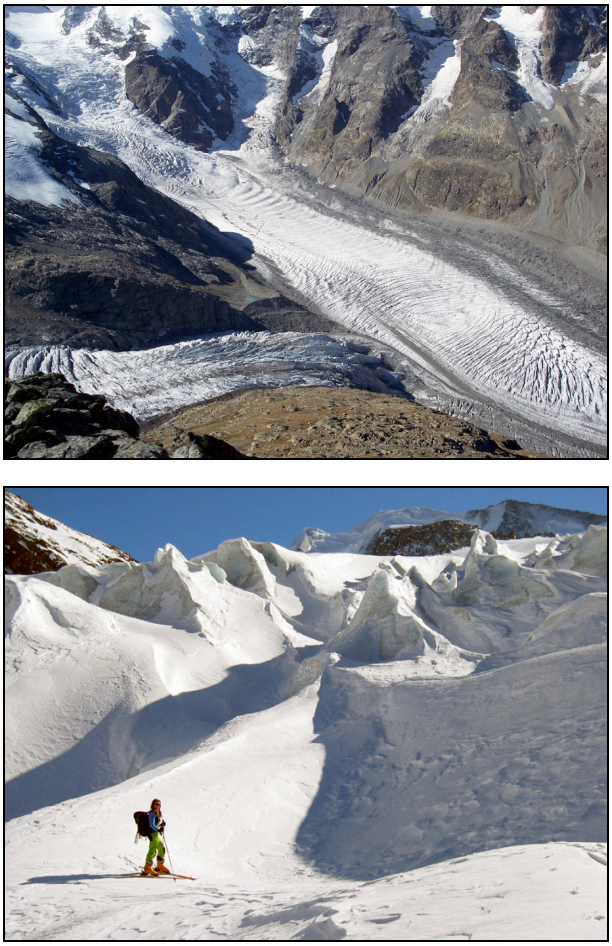

Figure 4. Microtopography due to the flow of ice. Crevasse patterns lead to strong spatial variability in the topographic rouhgness (Morteratschgletscher with an alumnus of the Karthaus summer school).

On a glacier, σ_{surf} varies strongly in space and time. In winter and spring, when snow covers the entire glacier, the surface is relatively smooth and σ_{surf} may have a typical value of 0.1 m or less. When the snow melts away on the lower part of the glacier, σ_{surf} will increase and may reach values of 0.5 m.

On valley glaciers the generation of microtopography by ice flow may be quite significant (*figure 4*). In crevassed regions the microtopography appears to be large, but is hard to quantify. Since crevasse patterns occur at certain places they create a substantial spatial variability in σ_{surf}. In view of this, it seems unlikely that atmospheric boundary layers over valley glaciers are in equilibrium with the local surface characteristics, because not too far upstream the microtop-ography may be quite different. The applicability of refined boundary-layer theories, defined and tested over large homogeneous terrain, is therefore very questionable. The simple scheme described above is more in keeping with our limited knowledge of the structure of turbulence over melting glaciers.

The previous discussion on turbulent fluxes has concentrated on the question of how fluxes can be calculated from measurements of wind, temperature and humidity at a given height. However, in studies of the response of glaciers to climate change the more important question is how the surface fluxes are related to the conditions in the free atmosphere. We cannot assume that in a world that is 1 K warmer the 2-metre temperature over a glacier will be 1 K higher. To gain some insight into this matter, at least in a qualitative sense, we will now discuss the simple glacier wind model originally developed by Prandtl (1942).

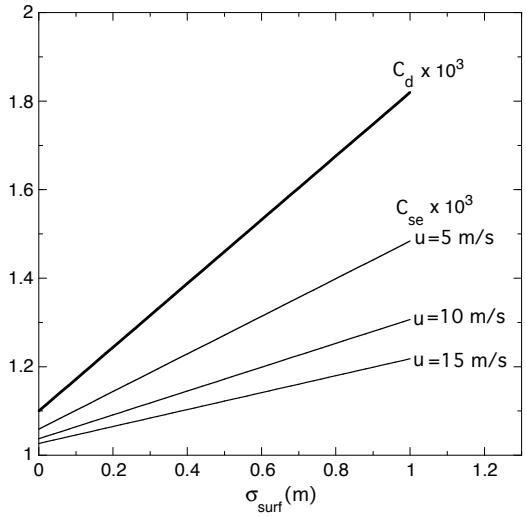

Figure 5. The relation between topographic roughness and exchange coefficients for momentum and heat.

3 A simple model of the glacier wind (Prandtl)

Before turning to the theory we look again at meteorological data obtained during the meteorological experiment on the Pasterze. *Figure 6* shows typical wind and temperature profiles obtained with a 13-m mast on which sensors were mounted at eight levels. At this site the slope of the glacier surface is about 5°. In this case, and in many other cases, the height of the wind maximum was between 2 and 8 m. The profiles are regular and the temperature variations are not large, in spite of the fact that at about 100 m above the surface the daily temperature range is about 10 K (this is known from balloon measurements). We conclude that the glacier wind has a well defined structure.

With regard to the dynamics of the glacier wind, the leading terms in the down-slope momentum budget are buoyancy forcing and friction. The leading terms in the heat budget are the sensible heat flux and vertical advection in the stably stratified atmosphere (Van den Broeke, 1997).

Direct heating of the air in the katabatic flow by radiation plays a minor role. We will now use these findings to formulate a simple model for the glacier wind.

First of all we define the x,z-coordinate system. We take z positive upwards perpendicular to the ice surface and x downwards parallel to the ice surface (*figure 7*). The wind velocity is parallel to the surface and denoted by u. The background atmosphere is stable and there are no horizontal temperature gradients. The stratification is denoted by γ, which is the vertical gradient of the reference potential temperature $\theta_0(z)$. The temperature relative to $\theta_0(z)$ is denoted by θ.

Next we formulate two coupled differential equations to be solved for the velocity and temperature profiles $u(z)$ and $\theta(z)$. The vertical component of the wind vector is $u \sin\eta$, so the local rate of heating due to downward vertical motion is given by $\gamma u \sin\eta$. The heat balance can then be written as:

$$\gamma u \sin\eta - \frac{\mathrm{d}F_{se}}{\mathrm{d}z} = 0 \qquad (3.1)$$

Here F_{se} is the turbulent flux of sensible heat (now positive upward !).

The (negative) buoyancy generated by the temperature deficit of the air near the glacier surface can be approximated as $g\theta/T_0$, where g is the acceleration of gravity and T_0 is a characteristic reference temperature (for instance the melting point). Balancing the buoyancy generation against the friction yields

$$\frac{\theta}{T_0} g \sin\eta + \frac{\mathrm{d}F_{mo}}{\mathrm{d}z} = 0 \qquad (3.2)$$

In fact, eqs. (3.1)-(3.2) form a reduced set of the more general equations for gravity flows (Mahrt, 1982).

We assume that the fluxes of heat and momentum can be described with K-theory (Stull, 1988):

$$F_{se} = K_{se} \frac{\mathrm{d}\theta}{\mathrm{d}z} \;\; ; \;\; F_{mo} = K_{mo} \frac{\mathrm{d}u}{\mathrm{d}z} \qquad (3.3)$$

Now K_{se} and K_{mo}, the eddy diffusivitites for heat and momentum, are assumed to be constant with z. The model then reduces to the classical Prandtl-model for slope winds (Prandtl, 1942). Note that this model cannot be valid close to the surface because in reality the eddy diffusivities go to zero. Nevertheless, it is an attractive model because it retains the coupling of the thermal and motion field, and it lets us obtain an analytical solution.

Combining eqs. (3.1)-(3.2) yields a 4th order equation for the temperature perturbation:

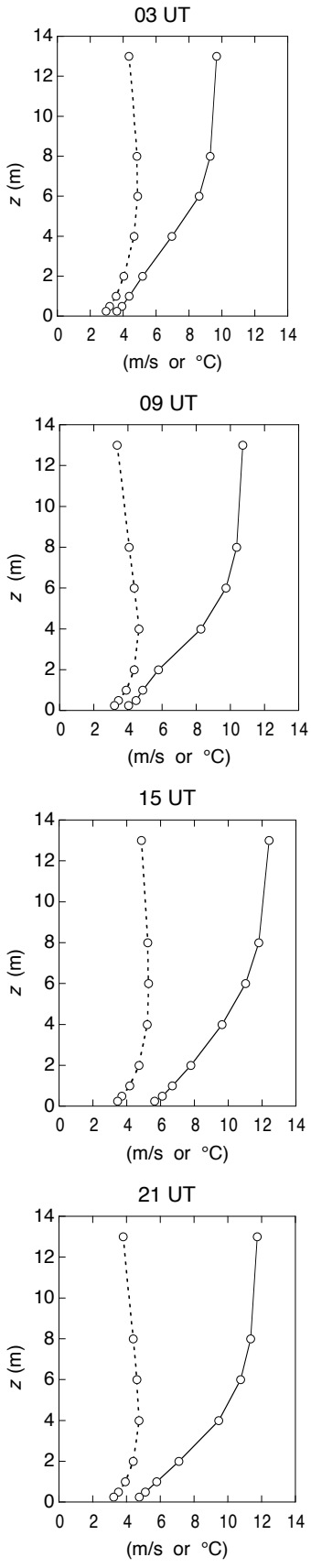

Figure 6. Measured profiles of temperature (solid) and wind speed (dashed) on a warm summer day during the Pasterze experiment (day 210, 1994). Each data point represents a 30 min average. Data provided by P. Smeets.

$$\frac{\mathrm{d}^4\theta}{\mathrm{d}z^4} + \frac{\gamma\, g \sin^2\eta}{T_0\, K_{mo}\, K_{se}}\theta = 0 \qquad (3.4)$$

Now boundary conditions have to be formulated. We require that the wind speed vanishes at the surface and that here the temperature perturbation equals C ($C < 0$). High above the glacier surface the wind speed and the temperature perturbation become zero. Therefore

$$z = 0 : u = 0 \text{ and } \theta = C \qquad (3.5)$$

$$z \to \infty : u = 0 \text{ and } \theta = 0 \qquad (3.6)$$

The solution fulfilling these conditions reads:

$$\theta = C\, \mathrm{e}^{-z/\lambda} \cos(z/\lambda) \qquad (3.7)$$

$$u = -C\,\mu\, e^{-z/\lambda} \sin(z/\lambda) \qquad (3.8)$$

where

$$\lambda = \sqrt[4]{\frac{4\,T_0\, K_{mo}\, K_{se}}{\gamma\, g \sin^2\eta}} \qquad (3.9)$$

$$\mu = \sqrt{\frac{g\, K_{se}}{T_0\, \gamma\, K_{mo}}} \qquad (3.10)$$

Here λ appears as the natural length scale of the flow. It increases with eddy diffusivity ($O^{1/2}$) and decreases with the temperature lapse rate ($O^{-1/4}$) and surface slope ($O^{1/2}$).
From eq. (3.8) we easily derive the height at which the wind maximum occurs:

$$z_m = \frac{\pi}{4}\lambda \qquad (3.11)$$

The maximum wind speed is:

$$u_m = -C\,\mu\, \mathrm{e}^{-\pi/4} \sin(\pi/4) \approx -0.322\, C\,\mu \qquad (3.12)$$

It should be noted that the maximum wind speed depends on the strength of the temperature forcing (C) and on K_{se}/K_{mo}, but not on the absolute values of the eddy diffusivities.
To plot the solution in non-dimensional form, one can scale temperature with C and wind speed with μC. The result is shown in *figure 9*. It can be seen that the basic structure of the glacier wind is present in the solution, which, given the simplicity of the model, is a nice result. However, in reality the temperature and wind velocity gradients close to the surface are much larger. Nevertheless, we analyse the solution of the Prandtl model a little bit further. The fluxes

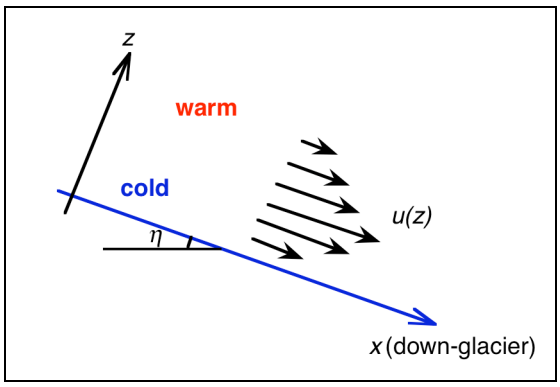

Figure 7. Coordinate system for a simple model of the glacier wind. The *x*-axis coincides with the glacier surface.

of momentum and sensible heat, F_{mo} and F_{se} respectively, are:

$$F_{mo} = \frac{\mu C K_{mo}}{\lambda} \, \mathrm{e}^{-z/\lambda} \, \left\{ \cos(z/\lambda) - \sin(z/\lambda) \right\} \qquad (3.13)$$

$$F_{se} = \frac{C K_{se}}{\lambda} \, \mathrm{e}^{-z/\lambda} \, \left\{ \cos(z/\lambda) + \sin(z/\lambda) \right\} \qquad (3.14)$$

The profiles are shown in *figure 10*. Of course, the momentum flux changes sign at the wind maximum because momentum has to be transported away from the jet. The momentum and heat fluxes, irrespective of the sign, have quite different shapes. The momentum flux increases more and more when we get closer to the surface, whereas the heat flux tends to a constant value. This is also seen in more sophisticated models and should be regarded as a typical feature of katabatic flow.

Several aspects of the Prandtl-model should be criticised. First of all, since eddy diffusivity does not decrease towards the surface, the steep velocity gradient close to the surface, normally formulated in the log or log-linear wind profile for a constant-flux layer, is not reproduced.

Secondly, in the model the katabatic jet is more pronounced that it is in reality (compare *figures 6* and *9*). The observed decrease in wind velocity with increasing height is much slower than in the model. This is in contrast to what one would expect. By using a constant eddy diffusivity it would be more logical to find a model jet that is too diffuse rather than too sharp.

A third feature not reproduced by the Prandtl-model is the increasing height of the wind maximum when the flow gets stronger (*figure 11*). A stronger glacier wind due to a larger thermal forcing corresponds to a larger (negative) value of C. However, eq. (3.12) shows that z_m does not depend on C, which is unrealistic. The reason for this discrepancy is obvious: stronger flow has better developed turbulence and the exchange coefficients in the model should be larger. This then would produce a larger value for z_m.

With regard to glacier mass-balance modelling the most important aspect of katabatic flow is the related surface heat flux delivering energy to the melt process. Because the forcing of the flow is temperature-dependent, it is likely that the surface heat flux will increase nonlinear with air temperature. In the next section a simple scaling model is discussed which deal with this aspect of the glacier wind.

4 Scaling of the glacier wind

In this approach no attempt is made to resolve the vertical structure of the glacier wind, but it is assumed that the heat and momentum balances are governed by eqs. (3.1)-(3.2),

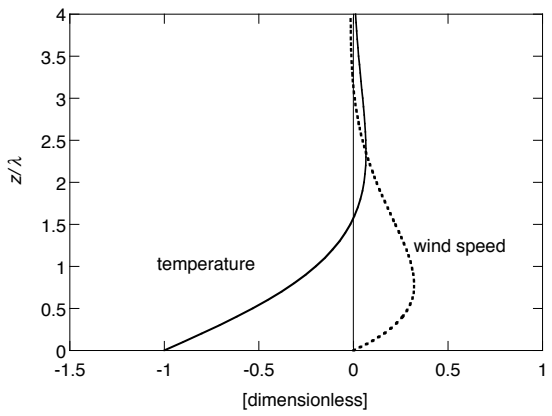

Figure 9. Dimensionless profiles of temperature and wind speed as predicted by the Prandtl model.

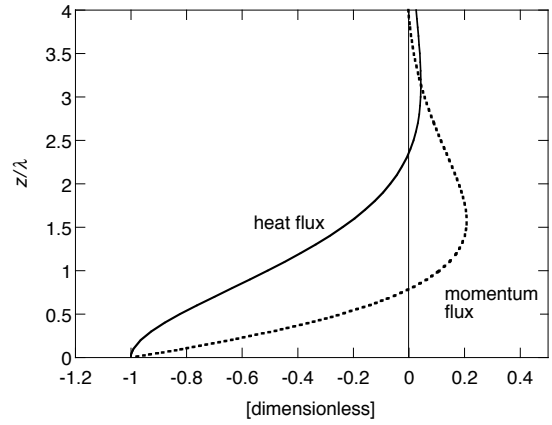

Figure 10. Dimensionless fluxes of momentum and sensible heat as predicted by the Prandtl model.

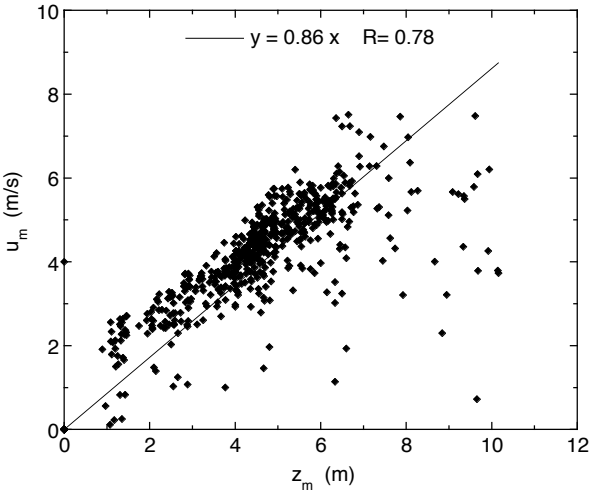

Figure 11. Scatter plot of height of the wind maximum (z_m) against strength of the wind maximum (u_m) for the glacier wind on the Pasterze glacier (data prepared by Bruce Denby; from Oerlemans and Grisogono, 2002).

and that the flow is characterised by a well defined wind maximum. To characterise the katabatic state we define scales for wind speed (u_s), temperature (θ_s) and length (z_s). We then obtain the following equations:

$$\gamma\, u_s \sin\eta - \frac{K_{se}\,\theta_s}{z_s^2} = 0 \tag{4.1}$$

$$\frac{\theta_s}{T_0}\, g \sin\eta + \frac{\mathrm{Pr}\, K_{se}\, u_s}{z_s^2} = 0 \tag{4.2}$$

Here the eddy Prandtl-number (K_{mo}/K_{se}) is denoted by Pr.
A further basic assumption is that the turbulence is generated by the glacier wind and consequently the eddy diffusivity for momentum should be expressed in the parameters describing the katabatic jet:

$$K_{mo} = k\, z_s\, u_s \tag{4.3}$$

Here k is a dimensionless constant. From eqs. (4.1)-(4.3) we can write

$$u_s = \theta_s \sqrt{\frac{g}{T_0\, \gamma\, \mathrm{Pr}}}\,, \quad z_s = \frac{k\theta_s}{\gamma \sin\eta} \tag{4.4}$$

The next step is to set the katabatic scales proportional to the maximum wind speed (u_m), the temperature deficit at the glacier surface (C), and the height of the wind maximum (z_m):

$$u_s = k_1\, u_m; \quad \theta_s = -k_2\, C; \quad z_s = k_3\, z_m \tag{4.5}$$

So from eq. (3.18) we have

$$u_m = \frac{k_2}{k_1}\, C \sqrt{\frac{g}{T_0\, \gamma\, \mathrm{Pr}}}\,, \quad z_m = -\frac{k\, k_2}{k_3}\, \frac{C}{\gamma \sin\eta} \tag{4.6}$$

So according to this model u_m and z_m increase linearly with the forcing -C, which is in agreement with the observations (note that in the original Prandtl model the maximum wind speed increases with -C while the height of the wind maximum is constant). The sensible heat flux at the glacier surface can be estimated as

$$F_{se} = -k\, k_2^2\, C^2 \sqrt{\frac{g}{T_0\, \gamma\, \mathrm{Pr}}} \tag{4.7}$$

Now a kind of 'heat pump' shows up: the sensible heat flux increases quadratically with the temperature difference between surface and air. The relation between u_m, z_m and F_{se} is shown in *figure 12*.

The rough ablation zone of Breidamerkurjökull, Iceland (find the person…)

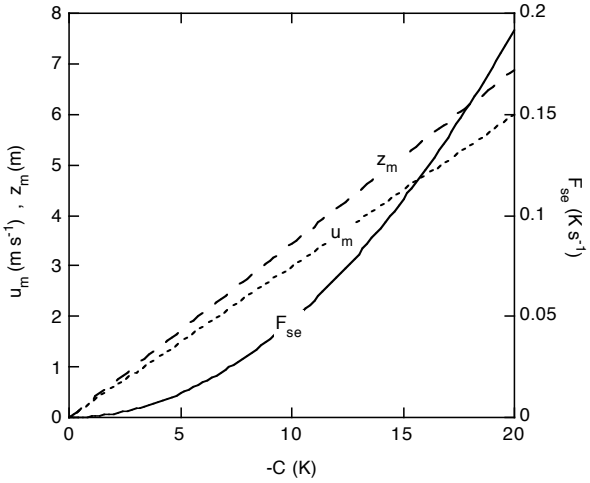

Figure 12. Height and strength of the wind maximum and associated surface sensible heat flux in relation to the forcing (temperature deficit) C, according to the model of section 4.4. Parameter values used: k_1=4, k_2=1, k_1=2.5, k=0.0004, Pr=5 (Oerlemans and Grisogono, 2002).

5 Micro-climate and large-scale weather

As discussed in section 3.6 the glacier micro-climate is embedded in a larger scale atmospheric system. We have seen that katabatic flow is relatively undisturbed by the large-scale flow. So the coupling of the glacier microclimate to the synoptic-scale weather conditions is likely to be determined by the temperature field. This point deserves further study, because in the end we want to relate the energy fluxes at the glacier surface to the large-scale meteorological variables.

The data set from the AWS on the Morteratschgletscher can be used to carry out a survey. It is fortunate that a number of synoptic weather stations (operated by the Swiss Meteorological Service) are located not too far from the Morteratschgletscher. We will look at data from Samedan, sometimes referred to as Sankt Moritz airport, and from Corvatsch. Samedan (1704 m) is located in the middle of a wide valley only 12 km north of the Morteratschgletscher. Corvatsch (3297 m) is a station close to a mountain top, at a distance of 9 km west of the Morteratschgletscher. These stations, being close to the Morteratschgletscher, are ideally suited for a comparison. We first look at a period of fair weather in October 1995 (*figure 13*).

The regularity of the temperature records is large. At Samedan the daily range is about 20 K, at the AWS about 6 K and at Corvatsch only a few degrees K. During this period the glacier wind blows steadily down the Morteratschgletscher, as shown in *figure 14*. Note that the wind speed closely follows air temperature through the day. The maximum wind speed lags behind the maximum temperature by a few hours.

The temperature observed at Samedan can be regarded as representative for the air filling the surrounding valleys. It can thus be used as a reference temperature for the katabatic forcing, i.e. it would correspond to a value of $|C|$ of about 13 K in the afternoon. Here a correction has been made for the altitude difference between Samedan and AWS Morteratsch by using a lapse rate of 0.007 K m^{-1}.

For a height of 3.5 m above the glacier, surface temperature and wind speed predicted by the modified Prandtl-model would be about 5 °C and 6 m s^{-1}. These numbers are for the parameter values that are given in the caption of *figure 12*. Apparently, the predicted wind speed is correct but the predicted temperature is too low. A better fit could be obtained by adjusting the parameters in the model, but this will not be discussed here.

It is also interesting to compare daily mean temperatures at these stations for a full year (*figure 15*). Clearly, a distinction should be made between the winter period (end of November until early March) and the rest of the year. For most of the year the correlation between the stations is very high, but in winter the temperatures for Samedan and the Morteratsch AWS tend to become decoupled. Samedan is in a wide flat valley and has much lower temperatures,

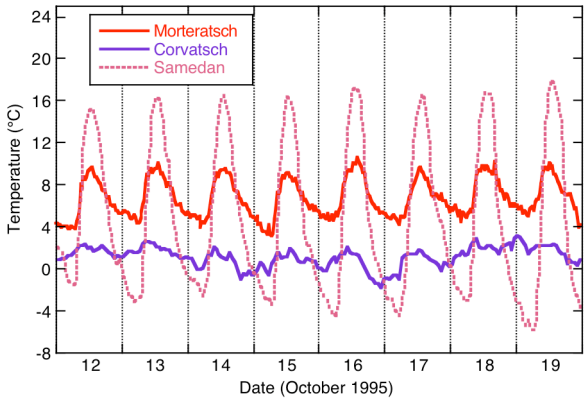

Figure 13. Air temperature measured at the Morteratsch AWS compared with observations at other stations.

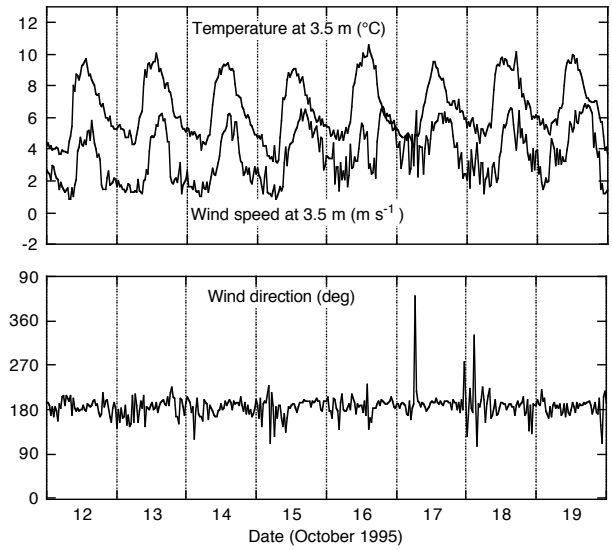

Figure 14. Air temperature measured at the Morteratsch AWS compared with observations of wind speed and wind direction.

especially during clear nights. This 'cold pool effect' is not present on the tongue of the Morteratschgletscher, where katabatic flow mixes warmer air downwards all the time.
The correlation coefficient between daily mean temperature at Corvatsch and the Morteratsch AWS is quite high: 0.97 on an annual basis. This result suggests that measurements from high-altitude weather stations are very valuable for estimating the temperature conditions over nearby glaciers ! Finally, it should be emphasised again that one must take great care when discussing air temperature over a melting glacier. Since the vertical temperature gradient is so large, the reference height should always be given!

References and further reading

Andreas E.L. (1987): A theory for the scalar roughness and the scalar transfer coefficients over snow and sea ice. *Boundary-Layer Meteorology* **38**, 159-184.

Banke E.G., S.D. Smith, R.J. Anderson (1980): Drag coefficients at AIDJEX from sonic anemometer measurements. In: *Sea Ice Processes and Models* (ed. R.S. Pritchard), Univ. of Washington Press, Seattle, 430-442.

Hoinkes H. (1954): Beiträge zur Kenntnis des Gletscher-windes. *Archiv für Meteorologie, Geophysik und Bioklimatologie* **B6**, 36-53.

Mahrt L.J. (1982): Momentum balance of gravity flows. *Journal of Atmospheric Sciences* **39**, 2701-2711.

Munro D.S., and J.A. Davies (1978): On fitting the log-linear model to wind speed and temperature proifles over a melting glacier. *Boundary-Layer Meteorology* **15**, 423-437.

Munro D.S. (1989): Surface roughness and bulk heat transfer on a glacier: comparison with eddy correlation. *Journal of Glaciology* **35** (121), 343-348.

Oerlemans J. and B. Grisogono (2002): Glacier wind and parameterisation of the related surface heat flux. *Tellus* **A 54**, 440-452.

Stull R.B. (1988): *An Introduction to Boundary Layer Meteorology*. Kluwer (Dordrecht), 666 pp.

Prandtl L. (1942): *Führer durch die Strömungslehre*. Vieweg u. Sohn, Braunschweig.

Van den Broeke, M.R. (1997): Momentum, heat and moisture budgets of the katabatic wind layer over a mid-latitude glacier in summer. *Journal of Applied Meteteorology* **36** (6), 763-774.

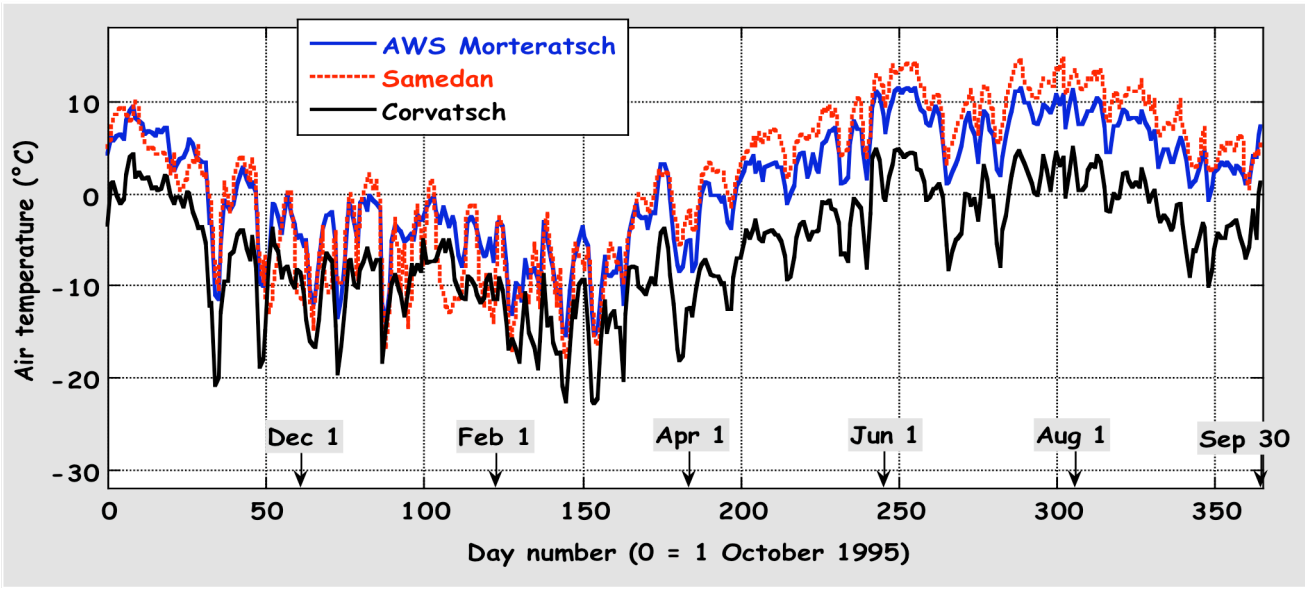

Figure 15. Daily mean air temperature for a full year measured on the Morteratschgletscher and surrounding stations.